

# Equilibrium Flow of a General Fluid Through a Cylindrical Tube

B. C. SAKIADIS

E. I. du Pont de Nemours and Company, Incorporated, Wilmington, Delaware

Equilibrium flow of a general fluid through a long, straight, cylindrical tube is examined, and equations are derived for determining the three pertinent material functions, the shear stress component, the difference between the radial and angular normal stress components, and the difference between the axial and angular normal stress components. These equations are expressed in terms of quantities which are measurable. Experimental data are obtained for a polymer solution, and the material functions are calculated.

The flow of non-Newtonian fluids through cylindrical tubes has been the object of numerous yet incomplete investigations. The approach taken in some of these investigations consists in assuming the form of the constitutive equations, which relate stress and rate of strain, solving these equations together with the force equations of motion for the particular flow motion considered, and subsequently fitting experimental measurements to the solution of the equations so as to obtain the material properties or numerical coefficients of the constitutive equations. This approach is limited by the nature of the assumptions made in formulating the constitutive equations. A more powerful approach in solving this problem consists in merely assuming the existence of general relationships between the stress and rate of strain components, then solving the stress equations of motion subject to certain physical restrictions, and subsequently utilizing the experimental measurements to determine the form of these general relationships. This approach appears to have been originated by Rabinowitch, as early as 1929 (1), specifically for the class of fluids which exhibit non-Newtonian but inelastic flow characteristics. Recently Coleman and Noll (2, 3) have formulated a general approach which applies to fluids exhibiting elastic flow characteristics as well, or general fluids, thus advancing toward some degree of completion.

The flow of a general fluid through a straight cylindrical tube, preceded by a larger approach channel, is quite complex. In this type of flow, which is quite common in practice, the fluid entering the tube is subjected to a higher level of shear than that existing in the approach channel. With general fluids exhibiting delayed response to stress or rate of strain, this flow situation results in large inlet pressure losses which extend far into the tube. These losses should not be confused

with the inertial effects which exist for all fluids. If the tube is sufficiently long, a point is reached when all stresses and the rate of strain are completely relaxed. Beyond this point the stresses and rate of strain do not vary with time or distance along the tube; that is the fluid has lost all memory of its prior flow history. Accordingly, the flow in this zone may be called *equilibrium flow* by analogy to thermodynamic nomenclature. Thus, in equilibrium flow\* the magnitude of the stresses and rate of strain depends only on the present state and the zero-shear isotropic state and not on the intervening flow history. Similarly the material properties exhibited in equilibrium flow may be called *equilibrium flow properties*.

Coleman and Noll (2) present solutions for a number of cases of equilibrium flow. In all cases the fluid is characterized in general by three material functions of the shear rate. These investigators however did not pursue the problem to its ultimate solution and gave no indication as to how two of the material functions are to be determined.

In the present investigation Coleman and Noll's results for flow through a straight cylindrical tube are extended, and relations are developed which when coupled with simple experimental measurements make it possible to determine for the first time, as far as is known, the material functions accurately and unambiguously. Flow through a cylindrical tube was chosen for this investigation because its flow symmetry eliminates the complicated side effects which exist in other flow problems. In the course of this investigation the behavior of the fluid in the jetting zone formed at the exit of the tube was studied and related to the flow conditions existing in the tube proper. Flow in these two zones is shown to be intimately related. The

\* An equivalent operational definition of equilibrium flow in channels is the presence of a constant pressure gradient along a flow line.

theoretical results are applied to measurements made with a polymer solution.

## THEORETICAL DEVELOPMENT

### Flow Problem

The motion considered is one in which a force is applied continuously, by a pump or some other device, causing a fluid to flow through a straight, vertical, cylindrical tube. At the exit of the tube the fluid is allowed to fall freely as a jet. With a given tube, and for each flow rate through the tube, provision is made to measure the following: the pressure as a function of distance at the tube wall, and the diameter profile of the fluid in the jetting section.

### Solution of Equations

The direction of motion of the fluid in the tube, relative to a stationary polar cylindrical coordinate system, is along the positive  $z$  axis, which coincides with the axis of the tube.

The following three assumptions, often realizable in practice, are made:

1. The fluid is homogeneous and incompressible. Nonmechanical effects are excluded from consideration.
2. The tube is sufficiently long so that equilibrium flow is attained at some distance from the inlet to the tube and persists thereafter. The present development deals with the flow in that section of the tube where equilibrium flow prevails, thus eliminating from consideration the inlet effects. Under these conditions the velocity field is independent of the  $z$  coordinate. The origin of the  $z$  coordinate is taken at the section of the onset of equilibrium flow.
3. The fluid velocity in the equilibrium flow section of the tube is a function of the radial coordinate  $r$  only; that is the flow is taken to be rectilinear.

In accordance with the above assumptions the only existing velocity component is  $v_z$ , and the only existing velocity gradient is  $dv_z/dr$ , both of which are functions of the  $r$  coordinate only. The only existing stress components are the normal stress components  $p_{rr}$ ,  $p_{\theta\theta}$ ,  $p_{zz}$ , and the shear stress component  $p_{rz}$  ( $= p_{rz}$ ). Further,

these stress components can be resolved as follows:

$$\left. \begin{aligned} p_{rr} &= p'_{rr} - p'' \\ p_{\phi\phi} &= p'_{\phi\phi} - p'' \\ p_{zz} &= p'_{zz} - p'' \\ p_{rz} &= p'_{rz} \end{aligned} \right\} \quad (1)$$

The stress components  $p'_{rr}$ ,  $p'_{\phi\phi}$ ,  $p'_{zz}$ , and  $p'_{rz}$  are functions of the  $r$  coordinate only, whereas  $p''$  is a function of both the  $r$  and  $z$  coordinates.

The dependence of the stress components on the  $r$  coordinate can be expressed equally well as a dependence on the velocity gradient, or shear rate,  $dv_z/dr$ . Accordingly one defines the following relations\*

$$\left. \begin{aligned} p_{rz} &= \tau \left( \frac{dv_z}{dr} \right) \\ p'_{rr} - p'_{\phi\phi} &= \sigma_1 \left( \frac{dv_z}{dr} \right) \\ p'_{zz} - p'_{\phi\phi} &= \sigma_2 \left( \frac{dv_z}{dr} \right) \end{aligned} \right\} \quad (2)$$

where  $\tau$ ,  $\sigma_1$ , and  $\sigma_2$  are functions of the velocity gradient  $dv_z/dr$  and remain to be determined. These functions are completely arbitrary, except for certain physical restrictions (2), and suffice to determine the history of motion of the fluid up to the hydrostatic pressure  $p''$ . These functions have been called (2) *material functions*, but may equally well be used to define equilibrium flow properties of the fluid as for example

$$\eta = \frac{\tau \left( \frac{dv_z}{dr} \right)}{\frac{dv_z}{dr}} \quad (3)$$

where  $\eta$  is another material function.

Equations (4) to (8) that follow were obtained by Coleman and Noll (2) by integration of the stress equations of motion

$$p_{rz} = -\frac{1}{2} ar = \tau \left( \frac{dv_z}{dr} \right) \quad (4)$$

which is inverted to

$$\frac{dv_z}{dr} = -\tau^{-1} \left( \frac{1}{2} ar \right) \quad (5)$$

$$v_z(r) = \int_r^R \tau^{-1} \left( \frac{1}{2} a\xi \right) d\xi \quad (6)$$

$$\tau^{-1} \left( \frac{1}{2} aR \right) = \frac{1}{\pi a^2 R^3} \frac{d}{da} [a^3 q(a)] \quad (7)$$

$$p_{rr} = az - \frac{\rho}{g_c} gz + \int_r^R \xi^{-1} \sigma_1 \left[ \tau^{-1} \left( \frac{1}{2} a\xi \right) \right] d\xi + c \quad (8)$$

Equations (4) and (5) relate the shear stress to the radial distance  $r$ . Equation (6) is an expression for the fluid velocity and involves the additional assumption that no slip flow occurs at the tube wall. Equation (7) relates the shear rate at the tube wall  $-\tau^{-1} \left( \frac{1}{2} aR \right)$  to the flow rate  $q$ . [see also Equation (5)]. Equation (8) is an expression for the radial normal stress component. In Equations (4) to (8) the parameter  $a$ , which is a constant for a given tube and a specified flow rate, represents the total applied force exerted on a column of fluid of unit volume, and may be called (2) the *driving force*.

#### Determination of the Parameter $a$

At some point  $z_1$  within the equilibrium flow zone and at the tube wall Equation (8) reduces to\*

$$-P_{Rz_1} = [p_{rr}]_{z_1} = az_1 - \frac{\rho}{g_c} gz_1 + c \quad (9)$$

where  $P_{Rz_1}$  is the pressure measured at that location. Similarly at some other point  $z_2$  ( $z_2 > z_1$ )

$$-P_{Rz_2} = [p_{rr}]_{z_2} = az_2 - \frac{\rho}{g_c} gz_2 + c \quad (10)$$

From Equations (9) and (10) one obtains an expression for  $a$ , in terms of readily measurable quantities, or

$$a = \frac{P_{Rz_1} - P_{Rz_2}}{z_2 - z_1} + \frac{\rho}{g_c} g \quad (11)$$

Thus the parameter  $a$  is seen to be the pressure gradient along a given fluid streamline. Furthermore on a plot of  $P_{Rz}$  vs.  $z$  the point of onset of equilibrium flow corresponds to the point at which the pressure becomes a linear function of distance.

Equation (7) can be expressed in a more convenient form as follows:

$$-\left[ \frac{dv_z}{dr} \right]_{r=R} = \left[ \frac{3n+1}{4n} \right] \left[ \frac{32q}{\pi D^3} \right] \quad (12)$$

where

$$n = \frac{d \ln a}{d \ln \frac{32q}{\pi D^3}} \quad (13)$$

and  $D = 2R$ . A plot of  $-\frac{1}{2} aR$  vs.

$-\left[ \frac{3n+1}{4n} \right] \left[ \frac{32q}{\pi D^3} \right]$  then simply represents the material function  $\tau$ .

#### Determination of the Material Function $\sigma_1$

For  $z = L$  Equation (8) becomes

$$[p_{rr}]_L = aL - \frac{\rho}{g_c} gL + \int_r^R \xi^{-1} \sigma_1$$

$$\left[ \tau^{-1} \left( \frac{1}{2} a\xi \right) \right] d\xi + c \quad (14)$$

At the tube wall Equation (14) reduces to

$$[p_{rr}]_L = aL - \frac{\rho}{g_c} gL + c \quad (15)$$

Combining Equations (14) and (15) and setting  $r = 0$  one obtains

$$[p_{r0}]_L = [p_{rR}]_L + \int_0^R \xi^{-1} \sigma_1 \left[ \tau^{-1} \left( \frac{1}{2} a\xi \right) \right] d\xi \quad (16)$$

Now at the tube axis  $dv_z/dr = 0$ ; hence

$$[p'_{r0}]_z = [p'_{rz}]_{r=0} = 0 \quad (17)$$

Further, from Equations (1) and (17) for  $z = L$  there results

$$[p_{r0}]_L = -[p'']_{r=0, L} = [p_{zL}]_{r=0} \equiv 0 \quad (18)$$

when one considers only gauge pressures. This means that the pressure at the center of the tube exit is made equal to atmospheric pressure, and this is a boundary condition which must be satisfied in the flow motion considered. Accordingly Equation (16) reduces to

$$P_{RL} = -[p_{rR}]_L = \int_0^R \xi^{-1} \sigma_1 \left[ \tau^{-1} \left( \frac{1}{2} a\xi \right) \right] d\xi \quad (19)$$

The radial pressure  $P_{RL}$  can be obtained by extrapolation to  $z = L$  of the pressures  $p_{Rz}$  measured along the tube wall. Equation (19) transforms to

$$P_{RL} = \int_0^{\frac{1}{2} aR} \xi^{-1} \sigma_1 [\tau^{-1}(\xi)] d\xi \quad (20)$$

by changing the variable of integration from  $r$  to  $\frac{1}{2} ar$ . Differentiation of Equation (20) with respect to the upper limit yields

$$\sigma_1 \left[ \tau^{-1} \left( \frac{1}{2} aR \right) \right] = \frac{dP_{RL}}{d \ln a} \quad (21)$$

A plot of  $dP_{RL}/d \ln a$  vs.  $\left[ \frac{dv_z}{dr} \right]_{r=R}$  then simply represents the material function  $\sigma_1$ .

#### Determination of the Material Function $\sigma_2$

One assumes that the material function  $\sigma_1$  has been determined; then combining Equations (1) and (2) one gets

$$p_{zz} = p_{rr} + \sigma_2 \left[ \tau^{-1} \left( \frac{1}{2} ar \right) \right] - \sigma_1 \left[ \tau^{-1} \left( \frac{1}{2} ar \right) \right] \quad (22)$$

Specifying that  $z = L$  and using Equations (14) and (15) together with Equation (22) one obtains

$$p_{zL} = [p_{rR}]_L$$

\* Throughout this paper quantities in round or square brackets following the  $\tau$ ,  $\sigma_1$ , and  $\sigma_2$  functions indicate variables of these functions.

\* A positive sign associated with a stress component indicates a tension. Stress components denoted by capital letters indicate quantities measurable by the observer.

$$\begin{aligned}
& + \int_r^R \xi^{-1} \sigma_1 \left[ \tau^{-1} \left( \frac{1}{2} a \xi \right) \right] d\xi \\
& + \sigma_2 \left[ \tau^{-1} \left( \frac{1}{2} a r \right) \right] \\
& - \sigma_1 \left[ \tau^{-1} \left( \frac{1}{2} a r \right) \right] \quad (23)
\end{aligned}$$

Multiplying Equation (23) by  $2\pi r$  and integrating from  $r = 0$  to  $r = R$  one gets

$$\begin{aligned}
2\pi \int_0^R p_{zL} r dr &= \pi R^2 [p_{rR}]_L \\
& + 2\pi \int_0^R \left\{ \int_r^R \xi^{-1} \sigma_1 \right. \\
& \left. \left[ \tau^{-1} \left( \frac{1}{2} a \xi \right) \right] d\xi \right\} r dr \\
& + 2\pi \int_0^R r \sigma_2 \left[ \tau^{-1} \left( \frac{1}{2} a r \right) \right] dr \\
& - 2\pi \int_0^R r \sigma_1 \left[ \tau^{-1} \left( \frac{1}{2} a r \right) \right] dr \quad (24)
\end{aligned}$$

Integrating the second term on the right-hand side of Equation (24) by parts and changing the variable of integration from  $r$  to  $\frac{1}{2} ar$  one obtains

$$\begin{aligned}
\int_0^{\frac{1}{2} aR} p_{zL} \xi d\xi &= \frac{a^2 R^2}{8} [p_{rR}]_L \\
& - \frac{1}{2} \int_0^{\frac{1}{2} aR} \xi \sigma_1 [\tau^{-1}(\xi)] d\xi \\
& + \int_0^{\frac{1}{2} aR} \xi \sigma_2 [\tau^{-1}(\xi)] d\xi \quad (25)
\end{aligned}$$

Finally, differentiating Equation (25) with respect to the upper limit and using Equation (21) one finds that

$$\begin{aligned}
\sigma_2 \left[ \tau^{-1} \left( \frac{1}{2} aR \right) \right] \\
= \sigma_1 \left[ \tau^{-1} \left( \frac{1}{2} aR \right) \right] + P_{RL} \\
+ \frac{4}{aR^2} \frac{d}{da} \left[ \int_0^{\frac{1}{2} aR} p_{zL} \xi d\xi \right] \quad (26)
\end{aligned}$$

The integral in the square brackets represents a tensile force over the entire cross section at the tube exit divided by  $8\pi/a^2$ . This quantity can be determined as follows.

#### Determination of the Tensile Force at the Tube Exit

A jet of an elastoviscous fluid issuing from a cylindrical tube is known to expand (4) so that its diameter is larger than the tube diameter. Applying the momentum theorem along the  $z$  coordinate across the region from the tube exit ( $z = 0$ ) to the point of maximum jet diameter ( $z = z_m$ ) and ne-

glecting air drag and surface tension effects one gets

$$\begin{aligned}
F &= F_m + J - J_m \\
& + \int_0^{z_m} \frac{\rho}{g_c} g A dz \quad (27)
\end{aligned}$$

where

$$\begin{aligned}
F &= 2\pi \int_0^R p_{zL} r dr \\
& = \frac{8\pi}{a^2} \int_0^{\frac{1}{2} aR} p_{zL} \xi d\xi,
\end{aligned}$$

total tensile force at  $z = 0$

$F_m$  = total tensile force at  $z = z_m$

$$\begin{aligned}
J &= 2\pi \frac{\rho}{g_c} \int_0^R r v_z^2 dr, \\
& \text{momentum flux at } z = 0
\end{aligned}$$

$$\begin{aligned}
J_m &= \frac{\rho}{g_c} \pi R_m^2 \bar{v}_{zm}^2, \\
& \text{momentum flux at } z = z_m
\end{aligned}$$

and the origin of the  $z$  coordinate has been shifted to the tube exit. In evaluating the momentum flux  $J_m$  the assumption has been made that at the point of maximum jet diameter the axial velocity component is independent of the  $r$  coordinate. This is equivalent to the assumption that in the region  $0 \leq z \leq z_m$  the shear rate relaxes as fast or faster than the associated tensile stresses. The validity of this assumption rests on experimental evidence that the jet diameter changes only slightly beyond its maximum value with increasing distance from the tube exit. The fluid at the point of maximum jet diameter is then considered to be in a completely relaxed state, and this also means that

$$F_m = 0 \quad (28)$$

The continuity equation becomes

$$q = \pi R_m^2 \bar{v}_{zm} = \pi R^2 \bar{v}_z \quad (29)$$

Substituting Equations (28) and (29) in Equation (27) one obtains

$$\begin{aligned}
\int_0^{\frac{1}{2} aR} p_{zL} \xi d\xi &= \frac{a^2}{8\pi} \left[ J - \frac{\rho q \bar{v}_z}{g_c \alpha} \right. \\
& \left. + \int_0^{z_m} \frac{\rho}{g_c} g A dz \right] \quad (30)
\end{aligned}$$

where  $\alpha = A_m/A$ .

If the jet diameter changes only slightly with increasing distance beyond the location of its maximum, then the integral representing the gravitational acceleration in Equation (30) can be neglected. In this case only the maximum diameter of the jet need be measured.

An upper estimate of the tensile force at the tube exit is obtained by neglecting the second and third terms in the square bracket of the right-hand side of Equation (30). Thus the total tensile force at the tube exit be-

comes equal to the momentum flux at that location. Since the velocity profile in flow of elastoviscous fluids through cylindrical tubes varies from nearly flat to parabolic, the upper value of the total tensile force is readily found to be

$$J = 2\pi \frac{\rho}{g_c} \int_0^R r v_z^2 dr = \frac{4}{3} \frac{\rho}{g_c} q \bar{v}_z \quad (31)$$

and this with a parabolic velocity profile. Experimental evidence presented in this paper, and also obtained by other investigators, indicates that the magnitude of this tensile force is much smaller than the excess pressure drop associated with the inlet effects. This implies that the third term on the right-hand side of Equation (26) is small by comparison with the other terms. In such cases the equation for the material function  $\sigma_2$  simplifies to

$$\begin{aligned}
\sigma_2 \left[ \tau^{-1} \left( \frac{1}{2} aR \right) \right] \\
= \sigma_1 \left[ \tau^{-1} \left( \frac{1}{2} aR \right) \right] + P_{RL} \quad (32)
\end{aligned}$$

Use of Equation (32), instead of the more complicated Equation (26), should be justified by comparing the magnitude of  $J$  as given by Equation (31) with the measured values of  $AP_{RL}$  for the same values of  $a$ . For purely viscous fluid  $\sigma_2 = \sigma_1$ .

The effect of material properties on the expansion of the fluid at the exit of the tube, with gravitational acceleration neglected is obtained by combining Equations (20), (25), and (30). The result is

$$\begin{aligned}
\frac{1}{\alpha} &= k - \frac{g_c}{\rho \bar{v}_z^2} \int_0^1 \left\{ 2\sigma_2 \left[ \tau^{-1} \left( \frac{1}{2} aR\xi \right) \right] \right. \\
& \left. - \left[ 1 + \frac{1}{\xi^2} \right] \right. \\
& \left. \sigma_1 \left[ \tau^{-1} \left( \frac{1}{2} aR\xi \right) \right] \right\} \xi d\xi \quad (33)
\end{aligned}$$

where  $k$  is the ratio of the actual momentum flux at the tube exit to the momentum flux that would be obtained at the tube exit with a flat velocity profile, so that

$$\begin{aligned}
(\text{flat profile}) \quad 1 \leq k \leq \frac{4}{3} \\
(\text{parabolic profile})
\end{aligned}$$

#### Discussion

Equation (7) or Equation (12) which is the key equation in determining the material function  $\tau$ , was essentially developed as early as 1929 by Rabinowitch, as discussed in more recent references (1). There is however an important difference: the pressure gradient should be determined along a given fluid streamline as

shown in Equation (11), and not from measurements of the mean pressures across the entire tube section.

In accordance with Equation (27) the expansion of the fluid at the exit of the tube is due to the existence of a tensile force along the flow lines at the tube exit. The relaxation of this tensile force determines the profile of the expanding fluid jet.

The requirement for fluid expansion at the tube exit is obtained as follows. When one takes  $\sigma_1$  and  $\sigma_2$

$$\sim \left[ \frac{dv_z}{dr} \right]^2, \left[ \frac{dv_z}{dr} \right]_{r=R}$$

$$\text{and} \quad \sim \bar{v}_z \left[ \frac{3n+1}{4n} \right]$$

$$\left[ \frac{dv_z}{dr} \right]^2 / \left[ \frac{dv_z}{dr} \right]_{r=R}^2 \sim \xi^2$$

then the second term on the right-hand side of Equation (33) becomes

$$\sim \frac{1}{D^2} \left[ \frac{3n+1}{4n} \right]^2 \int_0^1 \xi^2 \left[ 2s - 1 - \frac{1}{\xi^2} \right] d\xi$$

where  $s = \sigma_2/\sigma_1$ . Fluid expansion is then obtained when  $s > \frac{3}{2}$ , which indicates that  $p'_{zz} > p'_{rr}$ . A plot of  $\alpha$  vs.  $\frac{1}{2} aR$  will not in general be unique for all tube diameters. Furthermore the existence of a maximum in such a plot appears possible. For a purely viscous fluid  $1/\alpha = k$ .

## EXPERIMENTAL WORK

### Apparatus and Instrumentation

A gear pump coupled to a variable-speed drive is used to pump the fluid from a supply tank through a header and the test section. A schematic drawing of the header and test section is shown in Figure 1. The test section consists of a vertical cylindrical channel  $\frac{5}{8}$  in. in diam. and 30.4 in. long. The inlet to the test section is square (180 deg. included angle). In testing, the fluid leaving the test section is allowed to fall as a jet over a vertical distance of about 4 ft. The pressure at the wall of the test section is measured by temperature-compensated pressure pickups mounted in specially machined taps (see Figure 1) along the length of the test section. The face dimensions of the pickups are  $\frac{5}{8}$  in. in diam. and 0.259 in. deep. The pressure pickups are excited by 5-v. d.c. from a storage battery, and their output is fed into a multipoint recording potentiometer which has a sensitivity of 0.02 mv. for spans less than 8 mv. Provision is made for varying the zero-load reading of the pickups by use of external variable resistors. A large pressure gauge is also mounted on the header. The apparatus is run at room temperature.

### Test Fluid

The fluid used in the tests was a water solution of Elvanol polyvinyl alcohol of the following composition: 14.37% by weight of Elvanol, grade 72-60, with 0.2% by weight based on solids of Triton X-100 gel inhibitor.

### Experimental Procedure

The pressure pickups located near the inlet of the test section, and which read

the higher pressures, were calibrated in place statically before and after the series of tests against the pressure gauge in the header. The header pressure gauge was in turn calibrated separately against a dead-weight tester. The two pressure pickups located near the exit of the tube were calibrated in a separate stand against a calibrated pressure gauge. Pressures from these two pickups were computed by using the no-load reading obtained with the pickups mounted on the test section and the slope of their voltage-pressure characteristic lines obtained from the separate calibration

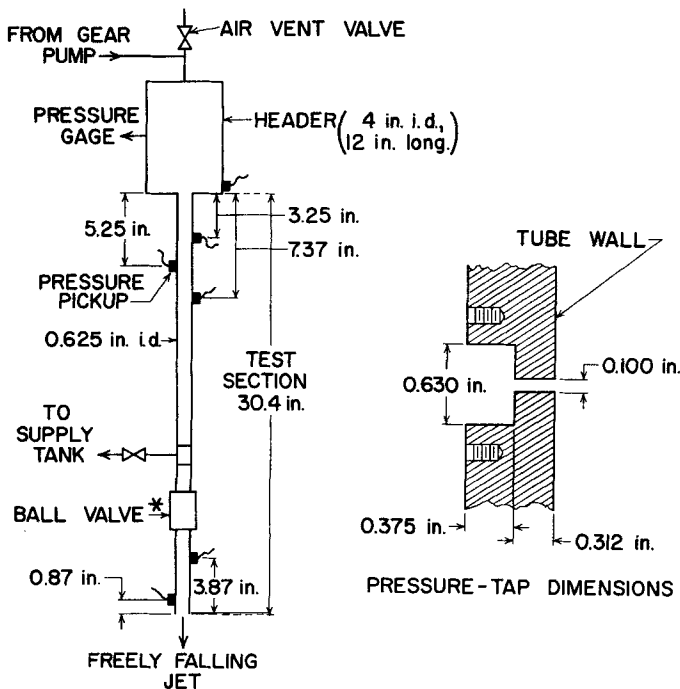
Prior to testing the fluid was circulated to expel air bubbles and to equalize its temperature. The flow rate was determined by collecting and weighing samples. The fluid density was 64.3 lb./cu. ft. The test temperature was 23°C.

Arrangements were made to photograph the falling jets so as to determine their diameter profiles from enlarged prints of the negatives.

The apparatus and procedure were checked by using a Newtonian fluid, corn syrup, prior to testing the Elvanol solution. For all flow rates the pressure readings were found to be linear functions of the tube length with negligible inlet effects. The pressure readings extrapolated to the tube exit indicated zero gauge pressures at that location. This is the behavior expected of a typical Newtonian fluid in highly viscous flow.

### Measurements and Computations

In Figure 2 is shown a plot of the pressure distribution at the tube wall for different flow rates. Such a plot, although helpful in showing trends, cannot be used directly to evaluate the normal pressures



\* Specially machined to conform with test tube.

Fig. 1. Apparatus.

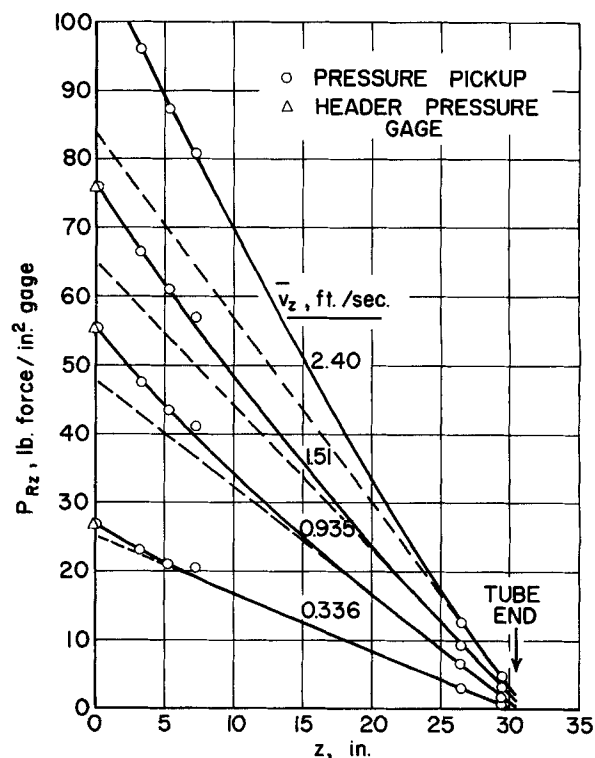


Fig. 2. Wall pressure vs. distance from tube inlet.

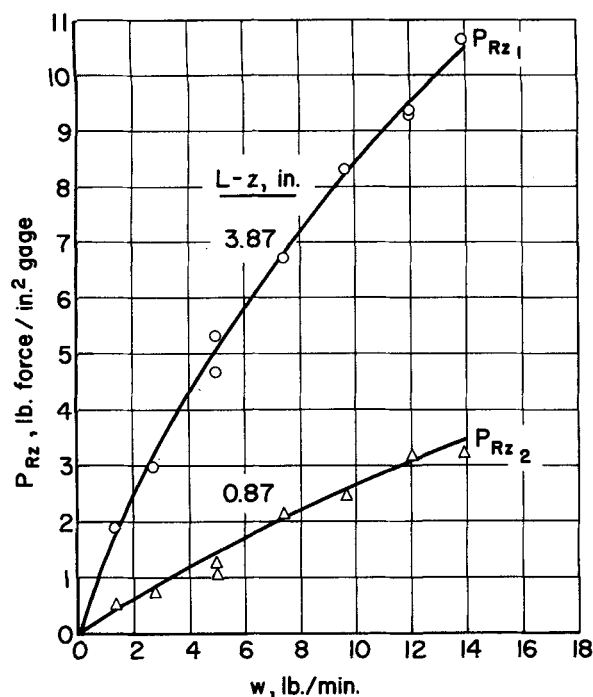


Fig. 3. Wall pressure vs. weight flow rate.

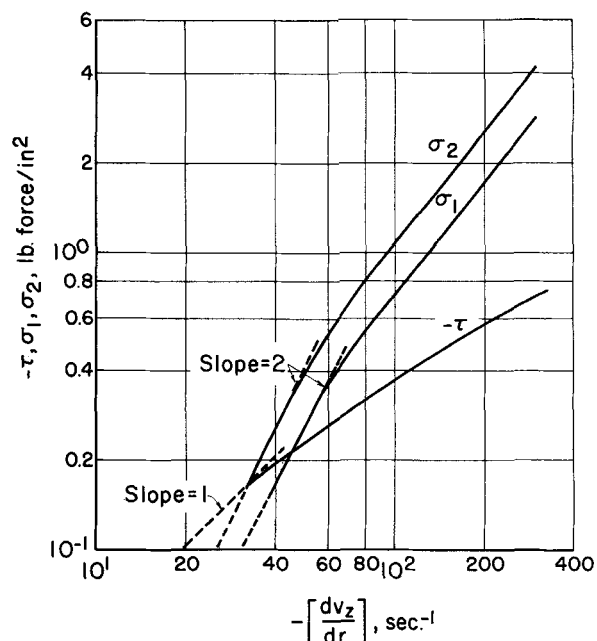


Fig. 4. Material functions of elvanol solution

at the tube exit. In Figure 3 is shown a plot of the pressures read by the two pickups located 3.87 and 0.87 in., respectively, from the tube exit vs. the weight flow rate. The curves through the data points are drawn so as to minimize the deviations. All subsequent computations are based on values read from the curves.

As seen in Figure 2 the pressure gradient is essentially constant near the exit of the tube. Thus the curves of Figure 3 represent, very nearly, equilibrium flow conditions. Equations (11), (12), (13), (21), and (32) were then used to compute the material functions,  $-\tau$ ,  $\sigma_1$ , and  $\sigma_2$  with curves of Figure 3. These functions are shown plotted vs. the shear rate in Figure 4. Equation (32), instead of Equation (26), was used in evaluating  $\sigma_2$  since the tensile stress  $J/A$ , as computed by Equation (3), was less than 4% of the pressure  $P_{RL}$  for all values of  $a$ .

#### Discussion

The results shown in Figure 4 indicate that the material functions  $\sigma_1$  and  $\sigma_2$  become increasingly important at the higher shear rates, as expected. At low shear rates  $\sigma_1$  and  $\sigma_2$  are quadratic functions of the shear rate as required (2). Further, at low shear rates the shear stress tends to become a linear function of the shear rate.

The tensile force  $F$  at the tube exit, although responsible for the jet expansion, does not contribute appreciably to the magnitude of the material function  $\sigma_2$ .

The developed equations permit the determination of the equilibrium flow properties of the fluid without introducing disturbances in the flow and with relatively simple apparatus. Owing to the axial symmetry of the flow field, edge effects are not present, thus eliminating sources of error common with rotational shear flow apparatus.

#### NOTATION

$A$	= cross-sectional area, sq. ft.
$a$	= driving force per unit volume in the direction of flow, lb.-force/(sq. ft.)(ft.)
$c$	= arbitrary constant, lb.-force/sq. ft.
$D$	= diameter, ft.
$F$	= total tensile force, lb.-force
$g$	= gravitational acceleration, ft./sec. <sup>2</sup>
$g_c$	= conversion factor, 32.2 (lb.)(ft.)/(lb.-force)(sec. <sup>2</sup> )
$J$	= momentum flux, lb.-force
$k$	= ratio of momentum fluxes, dimensionless
$L$	= specified tube length, ft.
$n$	= function defined by Equation (13), dimensionless
$P$	= pressure measured by observer at tube wall, lb.-force/sq. ft.
$p$	= stress component, lb.-force/sq. ft.
$p'$	= deviatoric stress component, lb.-force/sq. ft.
$p''$	= hydrostatic pressure, lb.-force/sq. ft.
$q$	= volumetric flow rate, cu. ft./sec.
$R$	= radius, ft.
$r$	= radial coordinate or radial distance from tube or jet axis, ft.
$s$	= ratio of material functions, dimensionless
$v_z$	= velocity component in $z$ direction, ft./sec.
$z$	= axial coordinate or axial distance, ft.

#### Greek Letters

$\alpha$	= $A_m/A$ , area ratio, dimensionless
$\eta$	= shear-dependent viscosity, (lb.-force)(sec.)/sq. ft.
$\xi$	= dummy variable, appropriate units
$\rho$	= fluid density, lb./cu. ft.
$\sigma_1$	= material function, lb.-force/sq. ft.
$\sigma_2$	= material function, lb.-force/sq. ft.
$\tau$	= shear stress, lb.-force/sq. ft.

#### Subscripts

$L$	= at tube exit
$m$	= at position of maximum jet diameter
$o$	= at tube or jet axis, or at origin of $z$ coordinate
$R$	= at tube wall
$r$	= in the $r$ direction, or at a radial distance, $r$
$z$	= in the $z$ direction, or at an axial distance, $z$
$\phi$	= in the azimuthal direction
1	= at $z = z_1$
2	= at $z = z_2$

#### Superscripts

-	= mean value
---	--------------

#### LITERATURE CITED

- Alves, G. E., D. F. Boucher, and R. L. Pigford, *Chem. Eng. Progr.*, **48**, 385 (1952).
- Coleman, B. D., and W. Noll, *Arch. Rat. Mech. Anal.*, **3**, 289 (1959).
- , *J. Appl. Phys.*, **30**, 1508 (1959).
- Metzner, A. B., E. L. Carley, and I. K. Park, *Modern Plastics*, **37**, 133 (1960).

Manuscript received June 5, 1961; revision received August 30, 1961; paper accepted August 31, 1961.